

# Colloidal Nanocrystals: A Toolbox for Materials Chemistry

Fabian Matter, Markus Niederberger, and Florian Putz\*

**Abstract:** Colloidal nanocrystals are the ideal building blocks for the fabrication of functional materials. Using various assembly, patterning or processing techniques, the nanocrystals can be arranged with unprecedented flexibility in 1-, 2- or 3-dimensional architectures over several orders of length scales, providing access to ordered or disordered, porous or non-porous, and simple as well as hierarchical structures. Careful selection of colloidal nanocrystals allows the properties of the final materials to be predefined. Moreover, by combining different nanocrystals, these properties can be fine-tuned for a specific application, opening up fascinating opportunities to create new materials for energy storage and conversion, catalysis, photocatalysis, biomedicine or optics. Indeed, functional materials made of preformed nanoparticles have been realized for metals, polymers, semiconductors, and ceramics, as well as for composites and organic-inorganic hybrids. In this review article, we introduce some concepts for the fabrication of colloidal nanocrystals and their assembly into dense and porous 3-dimensional structures. Porosity is a particularly important material property that strongly influences its application potential. Therefore, we pay special attention to this aspect and compare porous materials synthesized from nanoparticles with those from molecular routes. An additional focus is set on the degree of structural order that can be achieved on different length scales.

**Keywords:** Colloidal nanocrystals · Functional Materials · Materials chemistry



**Fabian Matter** is currently a PhD candidate in the Laboratory for Multifunctional Materials of Prof. Niederberger. He studied Interdisciplinary Science at the ETH Zurich and received his MSc degree majoring in inorganic chemistry and materials science in 2017. His research focus lies on the synthesis of highly crystalline nanoparticles and their assembly into aerogels for use in gas-phase catalysis.



**Florian Putz** is currently working as postdoc in the Laboratory for Multifunctional Materials of Prof. Markus Niederberger at ETH Zurich. He studied materials science at the Technical University of Munich and the Paris Lodron University of Salzburg, where he received his PhD in 2019. His research interests include the fabrication of hierarchically organized, porous materials with specifically designed microstructures and

complex macroscopic shapes that provide special functionalities for bioinspired and smart materials applications. He was granted a three-year Erwin Schrödinger Fellowship by the Austrian Science Fund for his current research project.



**Markus Niederberger** is head of the Laboratory for Multifunctional Materials and full professor at the Department of Materials at ETH Zurich. He studied chemistry at ETH Zurich, where he also received his PhD. After a postdoctoral stay at the University of California at Santa Barbara, he was group leader in the colloid department at the Max Planck Institute of Colloids and Interfaces in Potsdam. His

research interests focus on the development of liquid-phase synthesis routes to inorganic nanoparticles and their assembly and processing into macroscopic materials with tailored properties and functionalities for applications in energy storage and conversion.

## 1. Introduction

Nanoparticle research, in particular the field of colloidal nanocrystals, is a fascinating branch of science.<sup>[1]</sup> With their size- and shape-dependent properties, nanocrystals have been studied as versatile building blocks for new materials and devices for decades. Like LEGO® bricks they can be assembled into larger entities that cannot be produced by traditional molecular chemistry.<sup>[2]</sup> The uniqueness of materials design by assembling preformed building blocks lies in the modularity of the approach, *i.e.* by the possibility to divide the whole process into individual steps. In a first step, the nanoparticles are synthesized with the desired properties, and in a second step, the nanoparticles are arranged into a geometry that is suitable for the application. This two-step strategy allows to separately take advantage of the great know-how that exists in the field of nanoparticle synthesis as well as in the field of nanoparticle assembly. It is, for example, no problem to combine a non-aqueous nanoparticle synthesis with a water-based self-assembly process. The arrangement of nanoparticles leaves many possibilities for materials creation. Although starting from a limited number of building blocks, which are often rather common compounds like gold, titania or carbon, an infinite number

\*Correspondence: Dr. F. Putz, E-mail: florian.putz@mat.ethz.ch  
Laboratory for Multifunctional Materials, Department of Materials,  
ETH Zurich, Vladimir-Prelog-Weg 5, CH-8093 Zurich, Switzerland

of new architectures is accessible. Pores can be introduced, the material can be ordered or disordered and rather complex hierarchies can be achieved.<sup>[3]</sup> Fig. 1 displays the huge variety of structures that can be produced just from spherical building blocks, but nowadays nanocrystals are of course available in many other shapes,<sup>[4,5]</sup> introducing another degree of freedom.<sup>[6]</sup>

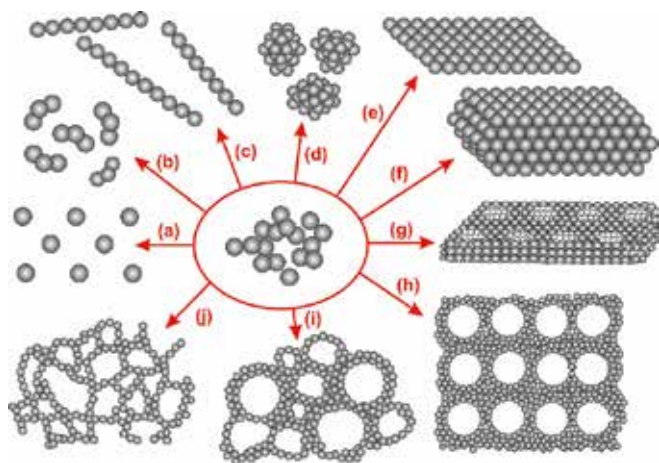


Fig. 1. Assembly of nanoparticles into a) single-particle arrays, b) colloidal molecules, c) 1D pearl-necklace structures, d) nanoparticle clusters, e) 2D monolayer arrays or thin films, f) 3D superlattices, g) (meso-) porous films, h) inverse opals, i) foams, and j) aerogels. Reproduced from ref. [3] with permission from Wiley-VCH.

From the synthesis point of view, but also regarding the assembly techniques, immense progress has been achieved in the last few years. However, one of the big challenges that remains is the size of the materials that can be produced by these approaches. While it is possible to get highly ordered materials on a small size scale, the order is typically lost when we go to macroscopic structures. One of the reasons for the difficulty to get ordered macroscopic structures is the fact that it is hard to control the interparticle interactions over several length scales. Understanding and mastering interparticle interactions such as van der Waals, electrostatic, magnetic, molecular and entropic forces is indispensable for large-scale assembly.<sup>[7,8]</sup>

In this review, we discuss the synthesis of defined nanoparticles and their arrangement into dense or porous and ordered or disordered materials such as supercrystals, inverse opals or nanoparticle-based aerogels. As porosity is a particularly interesting materials property, we put a special focus on that aspect by comparing porous nanoparticle assemblies with porous materials from molecular synthesis routes, and show possible strategies to create order on macroscopic length scales.

## 2. Particle Synthesis

Nanoparticles are typically synthesized by solid-state reactions, gas-phase routes or wet-chemical approaches.<sup>[9]</sup> Liquid-phase methods have the advantage of providing excellent control over particle size, size distribution, morphology and surface chemistry. Solution chemistry also offers many options for fine-tuning the composition, and in selected cases it is possible to rationally influence the crystal structure. Another major benefit of wet chemical synthesis methods is the facilitated transfer of nanoparticles into stable colloidal solutions. This is important for further processing, which in the most cases also takes place in liquid media.

The development of efficient synthesis routes has been at the heart of colloid science for several decades<sup>[10]</sup> and therefore an immense variety of liquid-phase methods for colloidal nanopar-

ticles is available.<sup>[11]</sup> At the same time, a few methods turned out to be particularly successful for a certain class of nanoparticles. For example, in the case of gold nanoparticles, the most widely used synthesis technique is the so-called citrate route developed by Turkevich *et al.* more than 60 years ago.<sup>[12]</sup> It is based on the reduction of gold chloride with sodium citrate, which also acts as stabilizing agent. Semiconducting nanoparticles are often produced by hot injection, a method introduced in 1993 by Murray, Norris and Bawendi for the production of high-quality CdE (E = S, Se, Te) quantum dots.<sup>[13]</sup> The synthesis involves the rapid injection of an organometallic precursor into a hot coordinating solvent, enabling the separation of nucleation and growth, which is the prerequisite to achieve a high degree of monodispersity. Among the different materials classes, metal oxides play an outstanding role from a scientific as well as from a technological point of view.<sup>[14]</sup> They offer an immense variety of structures, compositions and properties, which puts them in focus for many applications ranging from energy storage and conversion, catalysis and photocatalysis to sensing, optics or biomedicine.<sup>[15]</sup> Metal oxides are mainly prepared by sol-gel approaches, under hydrolytic as well as non-hydrolytic conditions. For colloidal metal oxide nanocrystals, non-aqueous sol-gel methods turned out to be particularly successful, mainly with respect to the high crystallinity of the particles, the accessibility of complex compositions and the ease of preparing colloidal dispersions.<sup>[16]</sup> Non-aqueous sol-gel routes involve the reaction of molecular precursors (*e.g.* metal halides, metal acetates, metal acetylacetonates, or metal alkoxides) with an organic solvent or a mixture of organic solvents with or without any surfactants, followed by heating in the temperature range of typically 50–250 °C (Fig. 2a).<sup>[17]</sup> Fig. 2b displays transmission electron microscopy overview images of different metal oxide nanoparticles with some of their properties. For doped metal oxide nanoparticles digital photographs of the colloidal dispersions and for tungsten oxide-poly(phenylene methylene) a bulk sample is shown. From a scientific point of view, a peculiar aspect of non-aqueous sol-gel chemistry is the fact that organic reactions are responsible for the formation of inorganic nanoparticles, which makes it possible to correlate the concepts of organic chemistry with nanoparticle synthesis, bringing some rationality to a field that has mainly been driven by trial-and-error experiments.<sup>[18]</sup>

For further processing of the nanoparticles into materials and devices, the nanocrystals must be present in colloidally stable dispersions, *i.e.* resisting agglomeration and gravitational settling.<sup>[19,20]</sup> Although wet chemical synthesis methods directly result in dispersions, the nanoparticles are usually still extracted from the reaction medium, because either the solvent is not suitable for the assembly experiment, or many other species are present in the synthesis mixture that could interfere with this subsequent step. The preparation of colloidally stable dispersions is generally trickier than one might think. Nanoparticles tend to agglomerate, and their surface chemistry must be carefully tuned to make them dispersible in a desired solvent. This is typically done by binding surfactants, polymers or charged ligands to the surface.<sup>[19,20]</sup> While such surface-adsorbed species are beneficial for the stability of the nanocrystals in dispersion, they can adversely affect the properties and function of nanocrystal-based materials and devices. Simple removal by heat treatment is often not possible, because sintering effects are not desired as they would destroy the nanoscale specific properties of the building blocks. Removal of organic residues has not been satisfactorily solved to date. In the next section, we move from the synthesis of nanoparticles to their colloidal assembly, beginning with a discussion of close-packed structures called colloidal crystals or superlattices.

## 3. Dense Colloidal Crystals

With the ability to synthesize monodisperse nanoparticles more than 30 years ago, also the idea of assembling them into

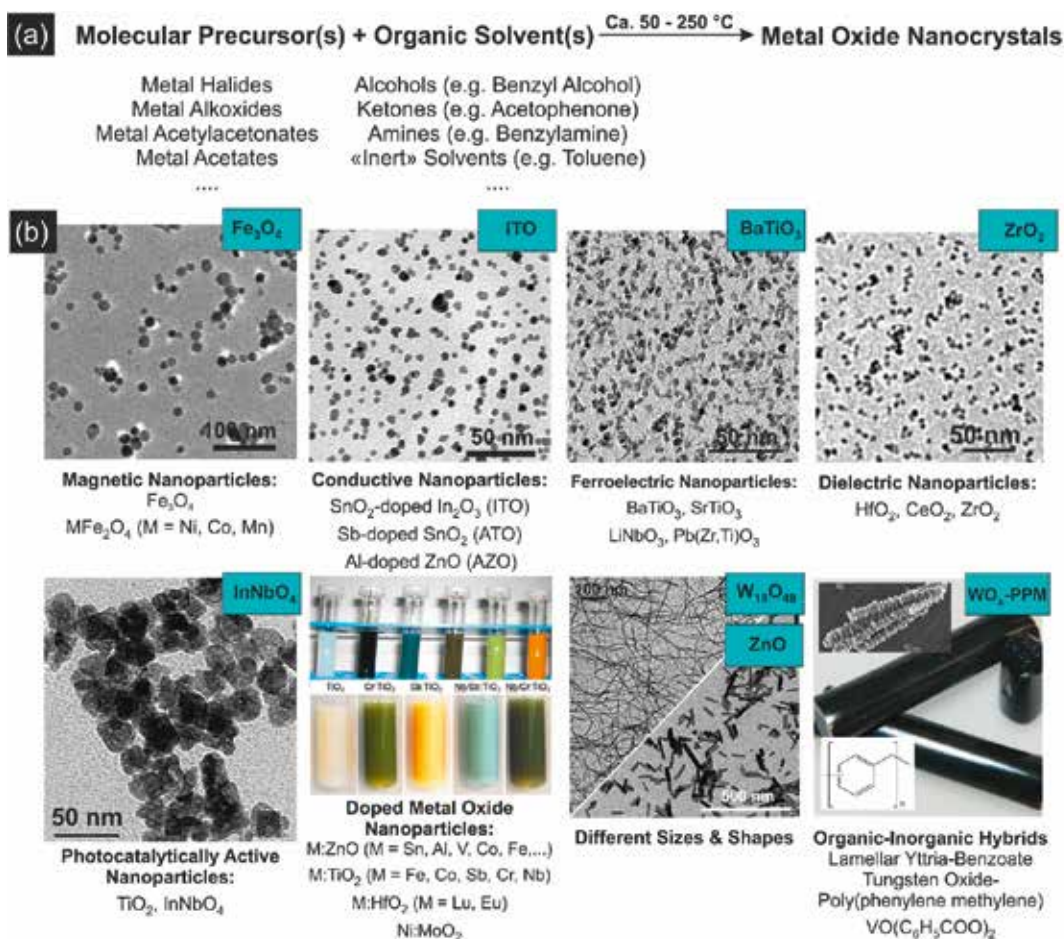


Fig. 2. (a) Schematic of the non-aqueous sol-gel synthesis approach to metal oxide nanoparticles using different precursor-solvent combinations.

(b) Transmission electron microscopy overview images of selected metal oxide nanoparticles with some of their properties and digital photographs of nanoparticle dispersions of doped metal oxide nanoparticles and of a bulk tungsten oxide-based hybrid.

ordered aggregates was developed.<sup>[21]</sup> Monodisperse iron oxide nanoparticles of 7 nm in size were obtained by the thermal decomposition of  $\text{Fe}(\text{CO})_5$  in decalin in presence of oleic acid – a process that is still used today in various modifications for the synthesis of iron oxide nanoparticles. After evaporation of the solvent, the nanoparticles assembled into micrometer-sized ‘supercrystals’ (today called superlattices). Several important concepts were already introduced in that paper. For example, the use of surfactants to control size, size distribution and agglomeration behavior was presented. Also the formation of ordered, close-packed structures as a result of the slow evaporation of the solvent and the narrow particle size distribution was discussed. Finally, the importance of van der Waals forces holding the nanoparticles together was also mentioned.

Emanating from these initial experiments involving isotropic assembly of just one type of nanoparticles into dense structures, the field has made immense progress, continuously increasing the complexity and intricacy of the assemblies, moving from ‘beautiful’ structures to functional materials and devices.<sup>[6,22]</sup> The structural variety ranges from colloidal molecules and patchy particles<sup>[23]</sup> to multi-component superstructures,<sup>[24]</sup> and chiral geometries,<sup>[25]</sup> including dense and non-dense packing, isotropic as well as anisotropic and ordered or disordered structures. While atoms remain the main building blocks of chemistry, these examples impressively illustrate that nanometer-sized objects can serve as superatomic building blocks, offering a powerful platform for materials chemistry to create analogous molecular or crystal-like structures. A particularly attractive feature of such assemblies lies in their collective properties, which differ from those of the individual nanoparticles or the corresponding bulk materials and arise as a result of the interaction between the nanocrystals. In this regard, the potential of colloidal crystals, superlattices, nanocrystal solids or supracrystals (they all refer to ordered arrays of

close-packed nanoparticles) for the generation of new materials has been recognized a long time ago.<sup>[26]</sup> The synthesis typically involves evaporation or destabilization of colloidal nanocrystal solutions, which induces the self-assembly of the nanoparticles in the crowded solution (Fig. 3a).<sup>[22]</sup> Evaporation can start from solutions that are drop-casted or doctor-bladed on a solid support, from small vials containing a substrate or from Langmuir-Blodgett films (Fig. 3a, left). Destabilization, on the other hand, is initiated by changing the polarity of the solvent by adding a non-solvent or by selectively removing the solvent from a solvent/non-solvent mixture (Fig. 3a, right). Gravitational sedimentation can also be applied for superlattice formation. By careful selection of the nanoparticles in the initial colloidal solution, the type of superlattice, its structure and its properties can be predefined. Taking advantage of the large pool of available nanoparticles covering a broad range of sizes, shapes and compositions, a whole library of superlattices has been reported.<sup>[22]</sup> For example, monodisperse PbS nanocrystals larger than 7 nm showed a strong tendency to form multiply twinned face-centered cubic superlattices with crystallographically forbidden five-fold symmetry elements (Fig. 3b,c).<sup>[27]</sup> If the colloidal nanocrystal solution is extended from one type of building block to a mixture of different nanocrystals, the diversity of accessible superlattices is increased. Fig. 3d,e shows the  $\text{AB}_2$  binary nanocrystal shape alloy superlattice with full positional order, which was obtained from a combination of nanorods and nanospheres. Depending on the aspect ratio of the rods and the size ratio of the rods to the spheres, different phases were observed.<sup>[28]</sup>

Superlattices are a popular example of densely packed nanocrystal assemblies. However, particle assembly can also be used to create a large variety of porous structures. Depending on the combination of pore sizes, such porous architectures can provide interesting additional features like a large accessible surface area,

an extremely low density compared to the corresponding bulk material, size and shape selectivity within the pores or mass transport throughout the material. The resulting materials properties are of potential benefit for applications in the fields of sorption, separation, catalysis, energy storage and conversion, sensing or biomedicine.<sup>[29]</sup> Porosity, whether it be ordered or disordered, can thus offer additional complexity as will be shown in the following sections.

#### 4. Ordered Porous Structures

The above-described synthesis routes towards colloidal nanoparticles or dense ordered structures can also be applied for the fabrication of porous materials with a great diversity regarding the pore size distribution in the meso- (pore sizes between 2–50 nm) or macropore (pores larger than 50 nm) regime and the structural order on the corresponding pore level.<sup>[3]</sup> While, for example, the direct assembly of preformed nanoparticles into porous structures typically results in materials with an undefined pore shape and a random pore arrangement (see Section 5), the use of 3D periodic assemblies of particles as template can yield porous structures with a high uniformity in pore size and shape as well as a periodic order of pores. Between these two extremes, a wide range of fine gradations in pore shape uniformity and structural periodicity and, correspondingly, various underlying synthesis strategies can be found.

To illustrate the large variety of synthesis approaches towards ordered porous structures on different length scales, a few molecular synthesis routes will also be shown in addition to the assembly of crystalline nanoparticles. On the side of porous structures with a well-defined pore shape, the light will be shed on three distinct types of meso- or macroporous materials with different degree of structural order: a) porous structures with defined, ordered pores, b) porous structures with ordered porous domains, and c) porous structures with defined, but disordered pores.

The first and structurally most ordered class of porous materials comprises so-called inverse opal structures (Fig. 1h).<sup>[30,31]</sup> This type of materials is characterized by a long-range, three-dimensional arrangement of highly uniform and typically spherical macropores. The synthesis is based on a templating approach, where 3D periodic arrangements of monodisperse particles, so-called opals, are used as template. These templates are then infiltrated by a second material that will later form the skeleton of the final product after the template is removed. The removal of the

template depends on the material used and can, for instance, be done by combustion or by etching. There is almost no limit to the chemical composition of inverse opals and many different organic and inorganic structures have already been synthesized.<sup>[32–35]</sup> Fig. 4 shows exemplary pore structures of copper (Fig. 4a) and carbon (Fig. 4b) inverse opals. Inverse opals with a pore size in the range of the visible wavelength show interesting optical properties and are therefore mostly applied as photonic crystals.<sup>[36–38]</sup> This is also the case for nanoparticle-based structures. For example, a macroporous semiconductor inverse opal can be prepared *via* the infiltration of close-packed silica spheres with CdSe quantum dots and subsequent removal of the template by hydrofluoric acid etching.<sup>[39]</sup> The optical properties of the resulting material can be further fine-tuned by an annealing step, which facilitates a transition from nanocrystal to semiconductor bulk characteristics. Beyond optics, the application field of inverse opals is quite diverse and reaches from electrodes for fast charging batteries over photoanodes for dye-sensitized solar cells to scaffolds for bone tissue engineering, to name just a few.<sup>[33,40,41]</sup>

If porous materials with a high specific surface area or size and shape selectivity are needed for a certain application, ordered porous structures with pores on a smaller length scale like the mesopore regime are favorable. In this case, liquid-crystalline phases of block copolymers can be used as templates.<sup>[29]</sup> For instance, porous tin oxide mesostructures with highly ordered pores in the range of 10–20 nm in diameter were synthesized by evaporation-induced self-assembly of tin oxide nanocrystals in the presence of polybutadiene-*block*- poly(ethylene oxide) in tetrahydrofuran.<sup>[42]</sup>

The mentioned techniques work very well on small length scales and are typically used in the synthesis of thin films with a high degree of structural order. However, the drawback of these approaches is the limited achievable sample size, as it becomes increasingly difficult to maintain a high pore order and a narrow pore size distribution when moving to larger dimensions.

In contrast to 3D periodic structures, certain materials do not exhibit a long-range order of pores, but only contain ordered domains of well-defined pores that, in turn, are randomly arranged throughout the material. The advantage of the underlying synthesis routes is their ability to form macroscopic objects produced as one continuous piece of material, so-called monoliths, which is challenging to achieve with completely ordered structures. An example for this type of materials are hierarchically structured, porous monoliths comprising domains of hexagonally arranged

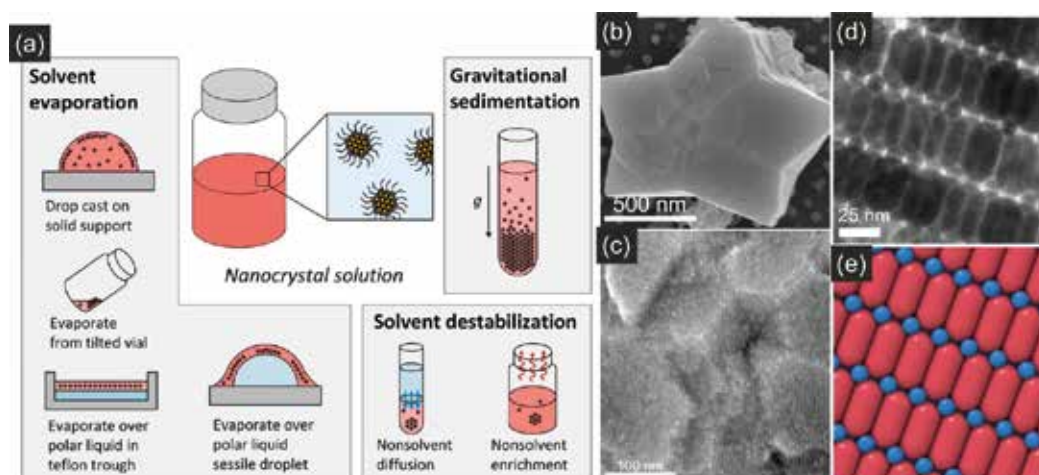


Fig. 3. (a) Overview of experimental approaches to nanocrystal superlattices involving evaporation (left) and destabilization or sedimentation techniques (right). Reproduced from ref. [22] with permission from the American Chemical Society. (b) Scanning electron microscopy image of a twinned PbS nanocrystal superlattice and (c) corresponding high-resolution image. Reproduced from ref. [27] with permission from the American Chemical Society. (d) Transmission electron microscopy image of an AB<sub>2</sub> binary nanocrystal superlattice composed of NaYF<sub>4</sub> nanorods and Fe<sub>3</sub>O<sub>4</sub> nanospheres and (e) its theoretical model structure. Reproduced from ref. [28] with permission from the American Chemical Society.

mesopores that show similarities to well-known mesoporous particle systems like SBA-15 or CMK-3.<sup>[46–48]</sup> In the case of silica, such architectures can be created by applying the sol-gel process of condensable silanes in combination with liquid-crystalline templating and polymerization-induced phase separation.<sup>[43,49]</sup> The resulting materials exhibit a macroporous network of struts, each strut containing cylindrical mesopores arranged on a 2D-hexagonal lattice (Fig. 4c). The network-constituting struts are in turn composed of the initial colloidal nanoparticles of the underlying sol-gel process. Taking this approach one step further, the as-synthesized silica materials can also act as porous hard templates for the fabrication of, *e.g.*, hierarchically structured porous carbon.<sup>[44]</sup> In this case, the network-constituting struts consist of hexagonally arranged carbon nanorods (Fig. 4d). In another variation of the fabrication route, the macroporous network of these silica or carbon materials can be modified to yield an anisotropic alignment of the struts *via* the application of mechanical forces in early stages of the synthesis.<sup>[43,44]</sup> The resulting porous architectures exhibit a preferential alignment of mesopores throughout the whole monolithic sample and thus an even higher degree of microstructural order (Fig. 4d). However, a long-range periodicity of pores, as can be found in the above-mentioned mesoporous thin films that are also templated with block copolymers, cannot be achieved by this approach. The ordered porous domains and especially their anisotropic arrangement in the macroscopic material can lead to interesting properties like the defined deformation of the ordered pore lattice and thus the whole monolith during fluid adsorption.<sup>[50–54]</sup> This effect could be used for sensing or actuation purposes or for so-called smart materials that change their shape depending on the surrounding conditions.

The third class of porous materials exhibits pores that are also well-defined in shape, but lack any periodic order, even over a short distance. Such architectures can be applied, if defined pores are needed, *e.g.* for encapsulation purposes, but a regular arrangement of the pores is only of minor importance. The big advantage of such assemblies are the underlying fabrication strategies, which are not only significantly simpler than strategies for highly ordered materials, but also allow for the fabrication of macroscopic samples.<sup>[55]</sup> Typical synthesis routes of such porous structures involve the application of monodisperse template particles that are coated with the target material and later removed in order to define the final pore shape.<sup>[3]</sup> In contrast to inverse opals, the template particles are not prearranged in a periodic way, but the assembly takes place in a random fashion after or concomitantly with the coating step. A class of materials where particle coating and assembly take place at the same time are so-called carbon spherogels, a special type of carbon aerogels that are solely composed of interconnected hollow spheres (Fig. 4e).<sup>[45]</sup> In this synthesis approach, monodisperse polystyrene spheres act as templates in the sol-gel processing of resorcinol-formaldehyde gels. The templates are subsequently removed during a carbonization step, which leaves behind a porous carbon network of hollow spheres with an extremely high shape uniformity.

As mentioned above, the coating and assembly of template particles can also be performed in two independent synthesis steps. An example of such a fabrication strategy is the synthesis of porous copper foam monoliths that are composed of hollow copper spheres (Fig. 4f).<sup>[55]</sup> In this case, the spherical zinc oxide particles used as templates are coated with copper and subsequently dissolved in formic acid. In the following step, hollow

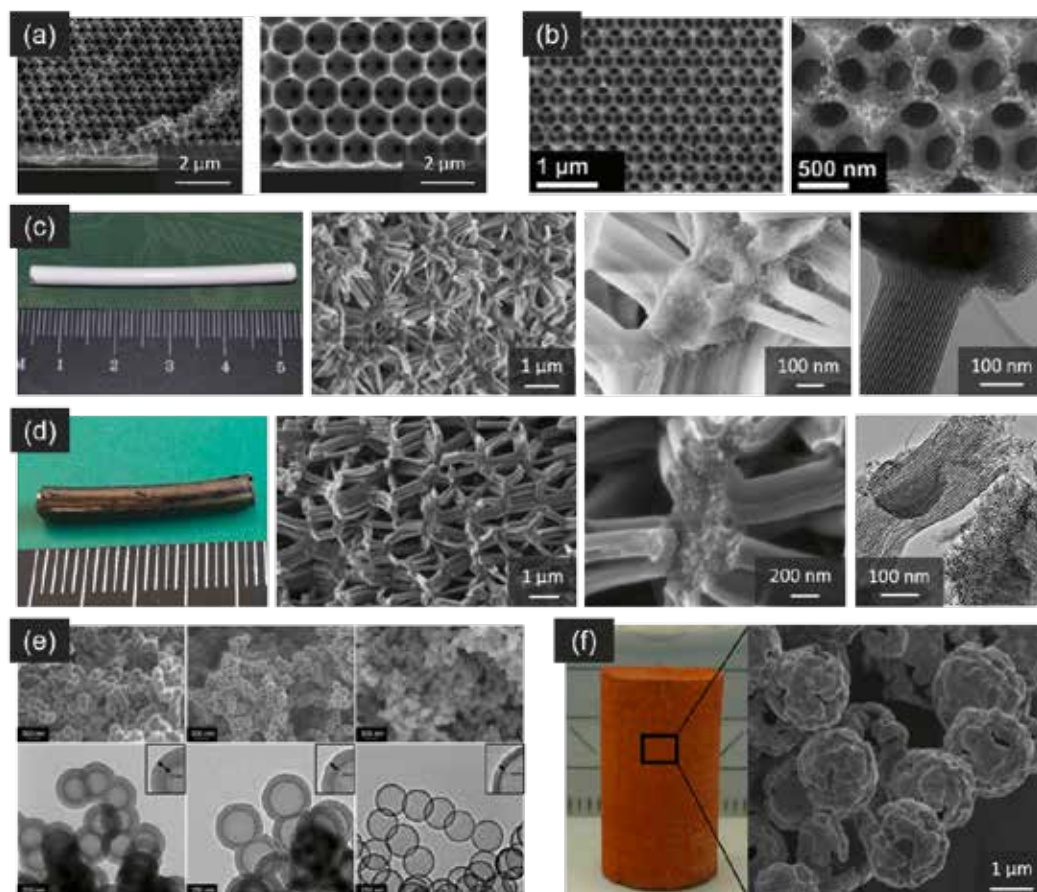


Fig. 4. (a) Scanning electron microscopy images showing the pore structure of copper inverse opals. Reproduced from ref. [34] with permission from Springer Nature. (b) Scanning electron microscopy images of the pore structure of carbon inverse opals. Reproduced from ref. [35] with permission from the Royal Society of Chemistry. (c) Photograph (left), scanning electron microscopy images (center) and transmission electron microscopy image (right) of hierarchically structured porous silica monoliths with ordered mesoporous domains. Reproduced from ref. [43] with permission from the American Chemical Society. (d) Photograph (left), scanning electron microscopy images (center) and transmission electron microscopy image (right) of hierarchically structured and anisotropic porous carbon monoliths with ordered mesoporous domains. Reproduced from ref. [44] with permission from the American Chemical Society. (e) Scanning electron micrographs of the pore structure of carbon spherogels. Reproduced from ref. [45] with permission from Elsevier. (f) Photograph (left) and scanning electron microscopy image (right) of a porous copper foam monolith.

copper spheres are assembled to form a copper foam monolith with defined pores but random pore arrangement.

Defined pores and an ordered pore arrangement can offer very special characteristics and functionalities, such as the optical properties of inverse opals or the deformation properties found in materials with ordered porous domains, which can be beneficial for a wide range of applications. However, there are also cases where structural order can be disadvantageous or simply unnecessary. One of the most striking types of disordered porous materials are aerogels. This class of materials has been available for several decades and exhibits a variety of unusual structural properties. Typically, sol-gel chemistry is used to fabricate such nanostructured materials. Recently, it has also become possible to fabricate similar structures by the assembly of preformed nanoparticles, which greatly expands the range of properties of this class of materials. In the following section, conventional aerogels with their advantages and disadvantages are compared with the emerging class of nanoparticle-based aerogels.

## 5. Disordered Porous Structures

Aerogels are highly porous, sponge-like materials that are made up of a disordered three-dimensional nanostructure. Those fascinating materials are derived from wet gels in which the liquid component of the gel has been replaced by a gas. The remaining finely branched backbone is typically only a few nanometers thick and spans pores of up to a few tens of nanometers in size. With a solid content often less than one percent by volume, aerogels are composed mainly of air and are thus among the lightest solids ever made. These ultralight materials not only possess an extremely intriguing appearance (Fig. 5), but also a number of remarkable structural properties giving them great prospects in various applications such as sensors, detectors, filters, thermal insulators, electronic devices and catalysis.<sup>[56–67]</sup>

With their extremely low thermal conductivity, aerogels are among the best insulation materials available.<sup>[68]</sup> The reason for this high thermal insulation lies in the finely branched nanostructure. The pores in aerogels are typically only a few tens of nanometers in size and are thus in the range of the mean free path length of gas molecules. Gas molecules enclosed in such small pores can hardly transfer their energy to neighboring molecules by collisions, which virtually eliminates heat transfer. Due to this exceptional property, low-weight aerogels have not only been applied in extraterrestrial expeditions (*e.g.* for the Mars rover),<sup>[69]</sup> but are also increasingly used in terrestrial applications, such as insulation for subsea pipelines or as insulation material for buildings.

The fine fiber-like solid structure enclosing the pores, on the other hand, is only a few nanometers thick. As a result, aerogels typically exhibit very high surface-to-volume ratios and can have a specific surface area of up to 1000 m<sup>2</sup>/g and more. Thanks to the open interconnected pore network, this surface is fully accessible to chemical compounds, which makes aerogels attractive for use as adsorbents, as storage media or for catalytic applications.

Another remarkable property is the low and tunable refractive index. While gases have a refractive index close to 1 at ambient pressure, most solids and liquids have a refractive index above 1.3. For aerogels, a material somewhere in between, the refractive index can be adjusted almost continuously by varying the density (*e.g.* between 1.0026 and 1.26 for silica aerogels).<sup>[70]</sup> Because of this unique feature, such aerogels are used in high energy physics experiments all around the world.<sup>[71]</sup>

Aerogels are among the most fascinating human-made materials due to their numerous extraordinary properties, however, they also have certain drawbacks. Owing to their very low solids content, for example, aerogels are usually very brittle and difficult to handle. Moreover, the manufacturing process of aerogels is typically time-consuming as it involves a number of steps, which are briefly explained below.

The production of aerogels was first described by Kistler almost 100 years ago.<sup>[72,73]</sup> As the name implies, aerogels are derived from wet gels in which the liquid component of the gel has been replaced by air. The removal of the pore fluid is done by special drying processes in order to preserve the filigree filamentous gel network. Conventional drying, *e.g.* by evaporation, is not suitable for this purpose, as strong capillary forces occur which cause the pore walls of the gel network to contract and collapse.

Instead, supercritical drying is commonly applied (Fig. 6). In this very gentle drying method, capillary forces are largely bypassed by bringing the pore liquid *via* its supercritical state into the gaseous form. Liquid CO<sub>2</sub> is particularly suitable because its supercritical point is at relatively low temperature and pressure (31 °C, 74 bar). To this end, the initial (often aqueous) pore fluid of the gel is first exchanged by an intermediate solvent (usually acetone or ethanol), which can then be completely replaced by liquid CO<sub>2</sub> in a closed pressure vessel. After increasing the temperature and reaching the supercritical point, the CO<sub>2</sub> is vented in the gaseous form leaving behind a finely branched three-dimensional network, which forms the basis of the very light and highly porous solid.

Although traditional aerogels are mostly made of silica, the underlying framework is not limited to this particular compound. In his first publication in the 1930s, Kistler already synthesized aerogels from silica, alumina, tin oxide, tungsten oxide, gelatin, agar, cellulose, and even egg albumin.<sup>[72]</sup> Aerogels can thus be made from virtually any substance, the only limitation being that the material of interest can be produced as a gel. The methods for preparing inorganic gels and aerogels are briefly discussed in the following paragraphs.

Conventional aerogels are typically produced by molecular routes using sol-gel chemistry (Fig. 7a). In such an approach, a molecular precursor (often a metal alkoxide) is first dissolved in a suitable solvent and, upon addition of water, undergoes a number of hydrolysis and condensation reactions to form a solution of primary particles, the so-called sol.<sup>[74,75]</sup> Under carefully adjusted reaction conditions, the primary particles further condensate and form a three-dimensional random gel network. The resulting wet



Fig. 5. Photographs of silica aerogels showing exceptional properties such as light weight and low thermal conductivity. The bluish haze, aerogels are often referred to as ‘frozen smoke’, is the result of Rayleigh scattering (Credit: (a, c) Courtesy NASA/JPL-Caltech, (b) Laboratory for Multifunctional Materials, ETH Zürich).

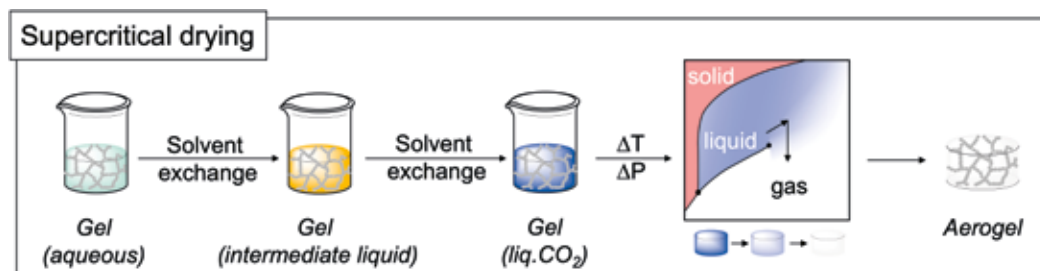


Fig. 6. Supercritical drying procedure of aqueous gels for the preparation of aerogels.

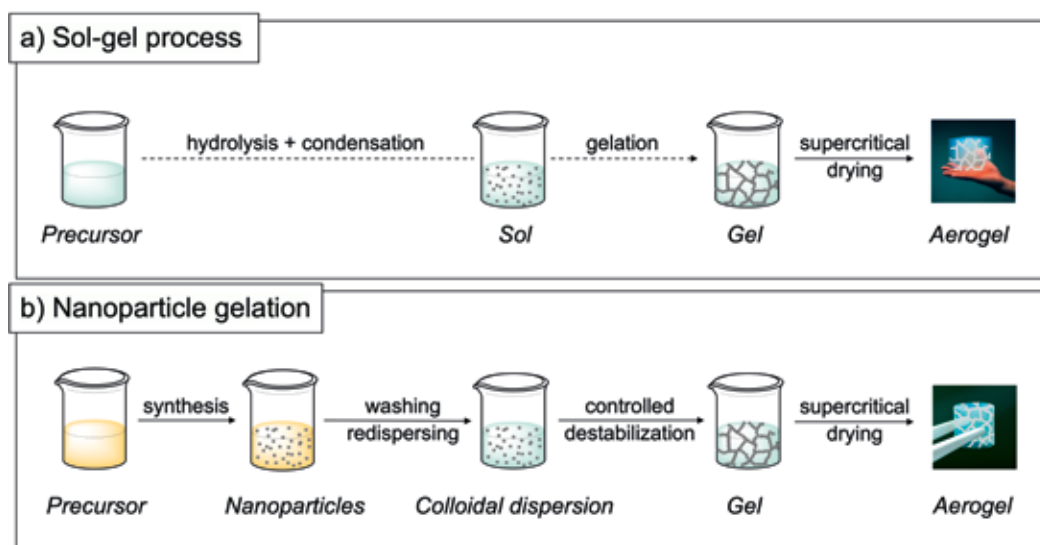


Fig. 7. Comparison of the conventional sol-gel process with the novel nanoparticle-based approach for the preparation of aerogels.

gel can be converted into an aerogel by means of supercritical drying. Many different metal oxides can be produced using traditional sol-gel chemistry and modifications of it including silica, alumina, zirconia, titania, chromia, yttria *etc.*<sup>[76,77]</sup>

The exceptional structural properties, such as high porosity, large internal surface area and low density, give sol-gel derived aerogels great prospects in many applications. Nevertheless, conventional aerogels still have a niche existence and are used, apart from some special applications, mainly as insulation materials. Besides the relatively high production costs, which are a general hurdle for large-scale production of aerogels, there are also limitations associated with the underlying sol-gel process. First, the hydrolysis and condensation are often very fast and hard to control, leading to aerogels with poor crystallinity. Although annealing could be applied to improve the crystallinity of an aerogel, such treatment is usually accompanied by severe changes in the nanostructured features that negatively affect both surface area and transparency. Moreover, the number of materials that can be accessed through the sol-gel chemistry is limited. The low crystallinity combined with the limited choice of materials makes it difficult to develop more sophisticated aerogel materials that not only offer all the unique structural advantages, but provide functionalities through a well-designed backbone material. A promising way to overcome the limitations of the sol-gel process is the use of preformed nanoparticles as building blocks in order to prepare nanoparticle-based aerogels.

Nanoparticle-based aerogels are a novel class of materials that combine the advantageous morphology of classical aerogels with features of nanocrystalline materials.<sup>[8,60,61,78–80]</sup> In contrast to the sol-gel approach, the formation of primary particles and their gelation proceed in two independent steps (Fig. 7b). First, surface-functionalized nanoparticles with a desired size, shape and composition are synthesized, washed and redispersed to form a stable colloidal solution. Second, the dispersion is destabilized in a con-

trolled manner to induce self-assembly of the nanocrystals into a three-dimensional gel network. Supercritical drying is finally applied to obtain a nanoparticle-based aerogel (also called nanocrystal aerogel). As the nanoscale properties of the initial building blocks are preserved in the macroscopic body, the nanoparticle assembling approach allows precise control over the composition and morphology of the resulting aerogel.

The concept of fabricating aerogels from preformed building blocks was first shown for CdS quantum dots in 2004.<sup>[88]</sup> Nowadays, a wide range of inorganic materials can be processed into nanoparticle-based aerogels including metal chalcogenides (CdS, CdSe, CdTe, PbS, ZnS, *etc.*),<sup>[84,88–96]</sup> metals (Pd, Pt, Au, Ag, *etc.*),<sup>[97–101]</sup> their oxides (TiO<sub>2</sub>,<sup>[102–106]</sup> Y<sub>2</sub>O<sub>3</sub>,<sup>[81]</sup> BaTiO<sub>3</sub>,<sup>[82]</sup> InTaO<sub>4</sub>,<sup>[107]</sup> SrTiO<sub>3</sub>,<sup>[87]</sup> Y<sub>3</sub>Al<sub>5</sub>O<sub>12</sub>,<sup>[108]</sup> *etc.*), nitrides (Cu<sub>3</sub>N),<sup>[83]</sup> phosphides (InP, Ni<sub>2</sub>P)<sup>[85,109]</sup> and fluorides (GdF<sub>3</sub>)<sup>[108]</sup> as well as combinations thereof (Fig. 8). The aerogels formed in this way not only offer high specific surface area and porosity, but also come along with the functional properties of their building blocks, such as photoluminescence, electrical conductivity, or photocatalytic activity, opening up completely new fields of application like sensing, electrocatalysis or photocatalysis. As different building blocks can be co-gelled in various combinations, multi-component aerogels with enhanced functionalities can easily be produced. Moreover, there are virtually no limits in the choice of building blocks. The preformed nanoparticles can be doped or undoped, highly crystalline or amorphous, have a single phase or core-shell structure, or can be spherical, rod-shaped or plate-like and so forth. By using such complex building blocks, highly sophisticated architectures can be realized that cannot be achieved with conventional sol-gel processes (Fig. 9). Nevertheless, there are some challenges that need to be overcome for a successful preparation of nanoparticle-based aerogels.

The preparation of highly concentrated and stable dispersions is one of the most challenging steps on the way to nanoparticle-

based aerogels. High concentrations (typically 20–200 mg/mL) are required to ensure network formation upon destabilization, while high colloidal stability is essential to prevent agglomeration and ensure uniform distribution of the nanometer-sized building blocks in the solution.<sup>[8]</sup> Larger compact agglomerates present in the initial dispersion are transferred into the final aerogel structure and affect the surface area, transparency and mechanical properties of the resulting aerogel. Surface modifications are typically applied, even during synthesis or in post-synthetic steps, in order to provide a good colloidal stability in the desired solvent.<sup>[113]</sup> The most common way is the introduction of surface charges to achieve electrostatic repulsion in aqueous systems or the use of long-chain ligands for steric stabilization in organic solvents. Particles with appropriate stabilization can be redispersed in high concentration directly after the washing step.<sup>[83]</sup> Alternatively, a stable dispersion with lower loading can be concentrated by means of centrifugal filtration,<sup>[97,100]</sup> dialysis and rotary evaporation.<sup>[108,110]</sup>

In a second step, the building blocks are assembled into a three-dimensional network by controlled destabilization of the colloidal dispersion. The correct balancing of the destabilization speed and strength is another critical step on the way to nanoparticle-based aerogels.<sup>[8]</sup> Very weak destabilization prevents network formation or leads to long gelation times of days to weeks, too strong destabilization, on the other hand, leads to precipitation of the particles.<sup>[108,114,115]</sup> The difficulty lies in finding a suitable trigger which, on the one hand, increases the total attraction just enough, and, on the other hand, acts uniformly over the entire volume. There are a variety of chemical and physical stimuli that can be used for this purpose. Controlled destabilization can be accomplished by

means of additives such as acids, bases, electrolytes,<sup>[99,110]</sup> complexing agents,<sup>[96,114–116]</sup> ligand strippers,<sup>[85,88,97]</sup> or non-solvents.<sup>[82,102–105,108]</sup> Another possibility is the use of non-additive triggers such as temperature,<sup>[82,83,100,102–105]</sup> irradiation,<sup>[84,106]</sup> mechanical methods such as centrifugation,<sup>[81,107,117]</sup> ultrasonic treatment,<sup>[82]</sup> or electrochemical methods.<sup>[118]</sup> The choice of trigger depends primarily on the type of stabilization (electrostatic or steric). Metal chalcogenide aerogels are typically prepared from non-aqueous dispersions of sterically stabilized nanoparticles. The assembly is initiated by oxidative ligand removal by addition of chemicals (*e.g.*  $\text{H}_2\text{O}_2$ ), illumination or electrochemical reactions. In contrast, most metal and metal oxide aerogels are prepared in aqueous systems, where an assembly is initiated by screening of the surface charge by addition of salts, by using charged linker ions or upon addition of non-solvent and heating.<sup>[8]</sup>

The possibility to rationally design nanoparticle-based aerogels opens the way for the development of novel functional materials with great perspective in a wide range of applications. Networks derived from metal chalcogenide gels, for example, are not only capable of removing heavy metal ions from polluted water but have also been successfully used for optical sensing of triethylamine or very recently for sensing nitrogen dioxide with an unprecedented combination of low detection limit and high speed.<sup>[94,118,119]</sup> The electrically conductive and finely branched backbone of metallic aerogels, on the other hand, lends itself perfectly to electrocatalytic applications, such as hydrogen production or fuel cells. The advantages of such structures over standard catalysts have already been demonstrated in several studies (*e.g.* for alcohol oxidation, oxygen and hydrogen evolution reactions and oxygen reduction reaction).<sup>[101,120–130]</sup> Moreover, metal oxide aerogels

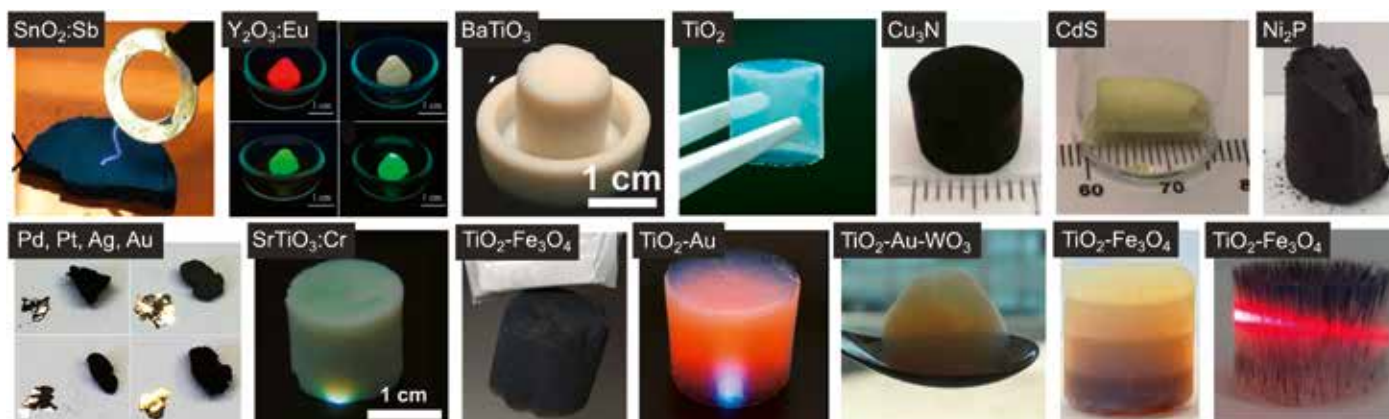


Fig. 8. Examples of nanoparticle-based aerogels. By the assembly of nanoscale building blocks, a variety of different materials can be processed into aerogels, including metals, metal oxides, nitrides, phosphides, chalcogenides. The co-gelling of different nanoparticles further allows the preparation of multi-component aerogels. Figures reprinted with permission from refs [78] ( $\text{SnO}_2\text{:Sb}$ ), [81] ( $\text{Y}_2\text{O}_3$ ), [82] ( $\text{BaTiO}_3$ ), [8] ( $\text{TiO}_2$ ), [83] ( $\text{Cu}_3\text{N}$ ), [84] ( $\text{CdS}$ ), [85] ( $\text{Ni}_2\text{P}$ ), [86] ( $\text{Pd}$ ,  $\text{Pt}$ ,  $\text{Ag}$ ,  $\text{Au}$ ), [87] ( $\text{SrTiO}_3$ ), [78] ( $\text{TiO}_2\text{-Fe}_3\text{O}_4$ ,  $\text{TiO}_2\text{-Au}$ ,  $\text{TiO}_2\text{-Au-WO}_3$ ).

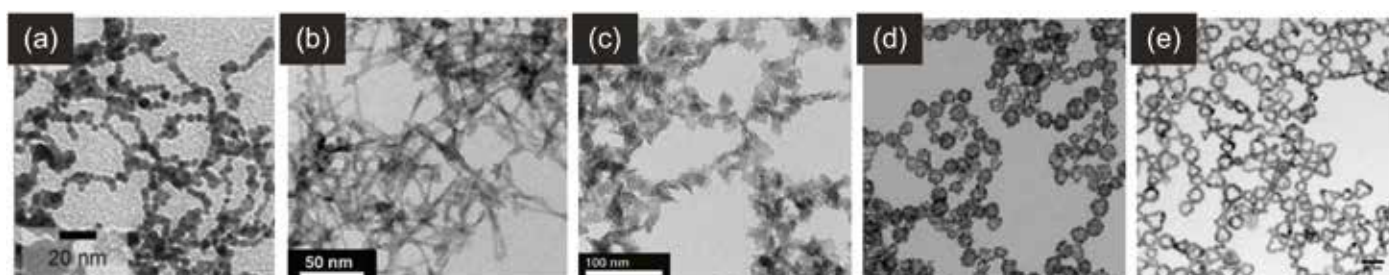


Fig. 9. Transmission electron microscopy images of nanoparticle-based aerogels composed of building blocks with different shapes. (a) Spherical co-assembled Ag and Au nanoparticles, (b) CdSe nanorods, (c) CdSe platelets, (d) PdNi hollow nanospheres, (e) Pt/Ag alloy nanoshells. Images reproduced from ref. [110] with permission from the American Chemical Society and from refs. [97,111,112] with permission from Wiley-VCH.

are considered extremely promising candidates for the development of (photo)catalysts for gas-phase reactions. By assembling highly crystalline TiO<sub>2</sub> nanoparticles, for example, transparent monolithic aerogels can be prepared that exhibit a large internal surface area (550 m<sup>2</sup>/g) and high porosity (99%). The photoactive backbone can further be fairly easily decorated with selected co-catalysts to enhance the performance. Such binary TiO<sub>2</sub>-metal aerogels have already been exploited in the photocatalytic conversion of gaseous CO<sub>2</sub><sup>[105]</sup> and also show surprisingly high activity in hydrogen production *via* methanol reforming.<sup>[106]</sup>

The preparation of aerogels from nanoscale building blocks is a relatively new approach that is still in its infancy. The rising knowledge about nanoparticle gelation, however, makes it possible to convert more and more materials into a highly porous form. The great successes recently achieved with such nanoparticle-based aerogel structures and the growing community suggest that there will be much to hear about this fascinating class of materials in the future.

## 6. Conclusions

Colloidal nanocrystals are a fascinating and highly versatile class of materials. They can be assembled over several length scales into a multitude of 1-, 2- or 3-dimensional, dense or porous, ordered or disordered architectures by various assembly or processing techniques, yielding a large variety of very special and unique materials properties.

The colloidal nanoparticles can be synthesized *via* solid-state reactions, gas-phase synthesis and wet-chemical methods, especially the latter providing excellent control over chemical composition, particle size, size distribution, morphology and surface chemistry or even the crystal structure. The deliberate assembly of as-prepared superatomic building blocks into larger entities, such as densely packed nanocrystal superlattices, can provide collective properties that are distinct from single nanoparticle or bulk characteristics. The introduction of porosity into nanocrystal arrangements can add further complexity to the resulting porous system. Highly ordered porous structures like inverse opals can be created by using 3D periodic arrangements of monodisperse particles as templates during nanoparticle assembly. While the underlying fabrication techniques are often limited to small sample sizes or thin films, monolithic materials with ordered porous domains and/or defined pore morphology can be achieved on the macroscopic scale by other synthesis procedures, especially molecular routes like sol-gel chemistry. The latter can also be seen as the traditional approach in the synthesis of aerogels, a class of disordered porous materials. More recently, an alternative approach has emerged, in which these highly porous materials have been assembled from colloidal nanocrystals, yielding so-called nanoparticle-based aerogels. There are certain challenges related to this approach, such as the preparation of highly concentrated and stable dispersions and correct balancing of the destabilization speed and strength. However, since virtually any combination of different nanocrystals can be co-gelled into multi-component aerogels, this approach provides also many opportunities for the creation of novel materials with enhanced functionalities. This again emphasizes the significance of colloidal nanocrystals as powerful toolbox for materials chemistry.

## Acknowledgments

Financial support by the Swiss National Science Foundation (Project 200021\_165888), the Austrian Science Fund FWF (Project J 4292-N36) and by ETH Zürich is gratefully acknowledged.

## Conflict of interest

The authors declare that they have no conflict of interest.

- [1] F. J. Heiligtag, M. Niederberger, *Mater. Today* **2013**, *16*, 262, <https://doi.org/10.1016/j.mattod.2013.07.004>
- [2] D. V. Talapin, *ACS Nano* **2008**, *2*, 1097, <https://doi.org/10.1021/nm8003179>
- [3] M. Niederberger, *Adv. Funct. Mater.* **2017**, *27*, 1703647, <https://doi.org/10.1002/adfm.201703647>
- [4] C. Burda, X. B. Chen, R. Narayanan, M. A. El-Sayed, *Chem. Rev.* **2005**, *105*, 1025, <https://doi.org/10.1021/cr030063a>
- [5] Z. H. Wu, S. L. Yang, W. Wu, *Nanoscale* **2016**, *8*, 1237, <https://doi.org/10.1039/C5NR07681A>
- [6] X. Bouju, E. Duguet, F. Gauffre, C. R. Henry, M. L. Kahn, P. Melinon, S. Ravaine, *Adv. Mater.* **2018**, *30*, e1706558, <https://doi.org/10.1002/adma.201706558>
- [7] K. J. M. Bishop, C. E. Wilmer, S. Soh, B. A. Grzybowski, *Small* **2009**, *5*, 1600, <https://doi.org/10.1002/smll.200900358>
- [8] F. Matter, A. L. Luna, M. Niederberger, *Nano Today* **2020**, *30*, 100827, <https://doi.org/10.1016/j.nantod.2019.100827>
- [9] U. Schubert, N. Hüsing, 'Synthesis of Inorganic Materials', 3rd ed., Wiley-VCH Verlag & Co. KGaA, Weinheim, **2012**.
- [10] E. Matijevic, *Chem. Mater.* **1993**, *5*, 412, <https://doi.org/10.1021/cm00028a004>
- [11] B. L. Cushing, V. L. Kolesnichenko, C. J. O'Connor, *Chem. Rev.* **2004**, *104*, 3893, <https://doi.org/10.1021/cr030027b>
- [12] J. Turkevich, P. C. Stevenson, J. Hiller, *Discuss. Faraday Soc.* **1951**, *11*, 55, <https://doi.org/10.1039/DF9511100055>
- [13] C. B. Murray, D. J. Norris, M. G. Bawendi, *J. Am. Chem. Soc.* **1993**, *115*, 8706, <https://doi.org/10.1021/ja00072a025>
- [14] D. Koziej, A. Lauria, M. Niederberger, *Adv. Mater.* **2014**, *26*, 235, <https://doi.org/10.1002/adma.201303161>
- [15] G. R. Patzke, Y. Zhou, R. Kontic, F. Conrad, *Angew. Chem. Int. Ed.* **2011**, *50*, 826, <https://doi.org/10.1002/anie.201000235>
- [16] R. Deshmukh, M. Niederberger, *Chem. Eur. J.* **2017**, *23*, 8542, <https://doi.org/10.1002/chem.201605957>
- [17] N. Pinna, M. Niederberger, *Angew. Chem. Int. Ed.* **2008**, *47*, 5292, <https://doi.org/10.1002/anie.200704541>
- [18] M. Niederberger, G. Garnweitner, *Chem. Eur. J.* **2006**, *12*, 7282, <https://doi.org/10.1002/chem.200600313>
- [19] Y. Yin, A. P. Alivisatos, *Nature* **2005**, *437*, 664, <https://doi.org/10.1038/nature04165>
- [20] M. A. Boles, D. Ling, T. Hyeon, D. V. Talapin, *Nat. Mater.* **2016**, *15*, 141, <https://doi.org/10.1038/nmat4526>
- [21] M. D. Bentzon, J. Vanwongergem, S. Morup, A. Tholen, C. J. W. Koch, *Philos. Mag. B* **1989**, *60*, 169.
- [22] M. A. Boles, M. Engel, D. V. Talapin, *Chem. Rev.* **2016**, *116*, 11220, <https://doi.org/10.1021/acs.chemrev.6b00196>
- [23] W. Y. Li, H. Palis, R. Merindol, J. Majimel, S. Ravaine, E. Duguet, *Chem. Soc. Rev.* **2020**, *49*, 1955, <https://doi.org/10.1039/C9CS00804G>
- [24] R. Tan, H. Zhu, C. Cao, O. Chen, *Nanoscale* **2016**, *8*, 9944, <https://doi.org/10.1039/C6NR01662F>
- [25] J. C. Fan, N. A. Kotov, *Adv. Mater.* **2020**, *32*, <https://doi.org/10.1002/adma.201906738>
- [26] M. P. Pileni, *Acc. Chem. Res.* **2007**, *40*, 685, <https://doi.org/10.1021/ar6000582>
- [27] S. M. Rupich, E. V. Shevchenko, M. I. Bodnarchuk, B. Lee, D. V. Talapin, *J. Am. Chem. Soc.* **2010**, *132*, 289, <https://doi.org/10.1021/ja9074425>
- [28] X. C. Ye, J. A. Millan, M. Engel, J. Chen, B. T. Diroll, S. C. Glotzer, C. B. Murray, *Nano Lett.* **2013**, *13*, 4980, <https://doi.org/10.1021/nl400653s>
- [29] A. Feinle, M. S. Elsaesser, N. Hüsing, *Chem. Soc. Rev.* **2016**, *45*, 3377, <https://doi.org/10.1039/C5CS00710K>
- [30] A. Stein, B. E. Wilson, S. G. Rudisill, *Chem. Soc. Rev.* **2013**, *42*, 2763, <https://doi.org/10.1039/C2CS35317B>
- [31] F. Meseguer, A. Blanco, H. Míguez, F. García-Santamaría, M. Ibasate, C. López, *Coll. Surf. A: Physicochem. Engin. Aspects* **2002**, *202*, 281, [https://doi.org/10.1016/S0927-7757\(01\)01084-6](https://doi.org/10.1016/S0927-7757(01)01084-6)
- [32] S. Kim, A. N. Mitropoulos, J. D. Spitzberg, H. Tao, D. L. Kaplan, F. G. Omenetto, *Nat. Photon.* **2012**, *6*, 818, <https://doi.org/10.1038/nphoton.2012.264>
- [33] M. R. Sommer, J. R. Vetsch, J. Leemann, R. Müller, A.R. Studart, S. Hofmann, *J. Biomed. Mater. Res. B: Appl. Biomater.* **2017**, *105*, 2074, <https://doi.org/10.1002/jbm.b.33737>
- [34] Q. N. Pham, M. T. Barako, J. Tice, Y. Won, *Sci. Rep.* **2017**, *7*, 10465, <https://doi.org/10.1038/s41598-017-10791-3>
- [35] D. McNulty, V. Landgraf, S. Trabesinger, *RSC Adv.* **2020**, *10*, 24108, <https://doi.org/10.1039/D0RA03693E>
- [36] R. C. Schroden, M. Al-Daous, C. F. Blanford, A. Stein, *Chem. Mater.* **2002**, *14*, 3305, <https://doi.org/10.1021/cm020100z>
- [37] G. I. N. Waterhouse, M. R. Waterland, *Polyhedron* **2007**, *26*, 356, <https://doi.org/10.1016/j.poly.2006.06.024U>
- [38] X. Yu, Y. J. Lee, R. Furstenberg, J. O. White, P. V. Braun, *Adv. Mater.* **2007**, *19*, 1689, <https://doi.org/10.1002/adma.200602792>

- [39] Y. A. Vlasov, N. Yao, D. J. Norris, *Adv. Mater.* **1999**, *11*, 165, [https://doi.org/10.1002/\(SICI\)1521-4095\(199902\)11:2<165::AID-ADMA165>3.0.CO;2-3](https://doi.org/10.1002/(SICI)1521-4095(199902)11:2<165::AID-ADMA165>3.0.CO;2-3)
- [40] H. Zhang, X. Yu, P. V. Braun, *Nat. Nanotechnol.* **2011**, *6*, 277, <https://doi.org/10.1038/nnano.2011.38>
- [41] P. Labouchere, A. K. Chandiran, T. Moehl, H. Harms, S. Chavhan, R. Tena-Zaera, M. K. Nazeeruddin, M. Graetzel, N. Tetreault, *Adv. Ener. Mater.* **2014**, *4*, 1400217, <https://doi.org/10.1002/aenm.201400217>
- [42] J. Ba, J. Polleux, M. Antonietti, M. Niederberger, *Adv. Mater.* **2005**, *17*, 2509, <https://doi.org/10.1002/adma.200501018>
- [43] F. Putz, R. Morak, M. S. Elsaesser, C. Balzer, S. Braxmeier, J. Bernardi, O. Paris, G. Reichenauer, N. Hüsing, *Chem. Mater.* **2017**, *29*, 7969, <https://doi.org/10.1021/acs.chemmater.7b03032>
- [44] F. Putz, L. Ludescher, M. S. Elsaesser, O. Paris, N. Hüsing, *Chem. Mater.* **2020**, *32*, 3944, <https://doi.org/10.1021/acs.chemmater.0c00302>
- [45] M. Salihovic, G. A. Zickler, G. Fritz-Popovski, M. Ulbricht, O. Paris, N. Hüsing, V. Presser, M. S. Elsaesser, *Carbon* **2019**, *153*, 189, <https://doi.org/10.1016/j.carbon.2019.06.086>
- [46] F. Putz, A. Waag, C. Balzer, S. Braxmeier, M. S. Elsaesser, L. Ludescher, O. Paris, W. J. Malfait, G. Reichenauer, N. Hüsing, *Micropor. Mesopor. Mater.* **2019**, *288*, 109578, <https://doi.org/10.1016/j.micromeso.2019.109578>
- [47] D. Zhao, J. Feng, Q. Huo, N. Melosh, G. H. Fredrickson, B. F. Chmelka, G. D. Stucky, *Science* **1998**, *279*, 548, <https://doi.org/10.1126/science.279.5350.548>
- [48] S. Jun, S. H. Joo, R. Ryoo, M. Kruk, M. Jaroniec, Z. Liu, T. Ohsuna, O. Terasaki, *J. Am. Chem. Soc.* **2000**, *122*, 10712, <https://doi.org/10.1021/ja002261e>
- [49] F. Putz, S. Scherer, M. Ober, R. Morak, O. Paris, N. Hüsing, *Adv. Mater. Technol.* **2018**, *3*, 1800060, <https://doi.org/10.1002/admt.201800060>
- [50] C. Balzer, A. M. Waag, S. Gehret, G. Reichenauer, F. Putz, N. Hüsing, O. Paris, N. Bernstein, G. Y. Gor, A. V. Neimark, *Langmuir* **2017**, *33*, 5592, <https://doi.org/10.1021/acs.langmuir.7b00468>
- [51] R. Morak, S. Braxmeier, L. Ludescher, F. Putz, S. Busch, N. Hüsing, G. Reichenauer, O. Paris, *J. Appl. Crystallogr.* **2017**, *50*, 1404, <https://doi.org/10.1107/S1600576717012274>
- [52] C. Balzer, A. M. Waag, F. Putz, N. Hüsing, O. Paris, G. Y. Gor, A. V. Neimark, G. Reichenauer, *Langmuir* **2019**, *35*, 2948, <https://doi.org/10.1021/acs.langmuir.8b03242>
- [53] L. Ludescher, R. Morak, C. Balzer, A. M. Waag, S. Braxmeier, F. Putz, S. Busch, G. Y. Gor, A. V. Neimark, N. Hüsing, G. Reichenauer, O. Paris, *Langmuir* **2019**, *35*, 11590, <https://doi.org/10.1021/acs.langmuir.9b01375>
- [54] L. Ludescher, R. Morak, S. Braxmeier, F. Putz, N. Hüsing, G. Reichenauer, O. Paris, *Phys. Chem. Chem. Phys.* **2020**, *22*, 12713, <https://doi.org/10.1039/D0CP01026J>
- [55] N. Kränzlin, M. Niederberger, *Adv. Mater.* **2013**, *25*, 5599, <https://doi.org/10.1002/adma.201301749>
- [56] J. E. Amonette, J. Matyas, *Micropor. Mesopor. Mater.* **2017**, *250*, 100, <https://doi.org/10.1016/j.micromeso.2017.04.055>
- [57] M. K. Carroll, A. M. Anderson, 'Aerogels as platforms for chemical sensors', in 'Aerogels Handbook', Eds. M. A. Aegerter, N. Leventis, M. M. Koebel, Springer, Dordrecht, **2011**, pp. 637-650.
- [58] W. Wan, R. Zhang, M. Ma, Y. Zhou, *J. Mater. Chem. A* **2018**, *6*, 754, <https://doi.org/10.1039/C7TA09227J>
- [59] H. Maleki, N. Hüsing, *Appl. Catal. B Environ.* **2018**, *221*, 530, <https://doi.org/10.1016/j.apcatb.2017.08.012>
- [60] C. Ziegler, A. Wolf, W. Liu, A.-K. Herrmann, N. Gaponik, A. Eychmüller, *Angew. Chem. Int. Ed.* **2017**, *56*, 13200, <https://doi.org/10.1002/anie.201611552>
- [61] B. Cai, A. Dianat, R. Hubner, W. Liu, D. Wen, A. Benad, L. Sonntag, T. Gemming, G. Cuniberti, A. Eychmüller, *Adv. Mater.* **2017**, *29*, 1605254, <https://doi.org/10.1002/adma.201605254>
- [62] W. Liu, A.-K. Herrmann, N. C. Bigall, P. Rodriguez, D. Wen, M. Oezaslan, T. J. Schmidt, N. Gaponik, A. Eychmüller, *Acc. Chem. Res.* **2015**, *48*, 154, <https://doi.org/10.1021/ar500237c>
- [63] A. Lukowiak, W. Strek, *J. Sol-Gel Sci. Techn.* **2009**, *50*, 201, <https://doi.org/10.1007/s10971-009-1952-z>
- [64] B. Cai, V. Sayevich, N. Gaponik, A. Eychmüller, *Adv. Mater.* **2018**, *30*, 1707518, <https://doi.org/10.1002/adma.201707518>
- [65] B. Cai, A. Eychmüller, *Adv. Mater.* **2019**, *31*, e1804881, <https://doi.org/10.1002/adma.201804881>
- [66] R. Du, X. Fan, X. Jin, R. Hübner, Y. Hu, A. Eychmüller, *Mater.* **2019**, *1*, 39, <https://doi.org/10.1016/j.matt.2019.05.006>
- [67] M. Schreck, M. Niederberger, *Chem. Mater.* **2019**, *31*, 597, <https://doi.org/10.1021/acs.chemmater.8b04444>
- [68] M. M. Koebel, A. Rigacci, P. Achard, 'Aerogels for Superinsulation: A Synoptic View', in 'Aerogels Handbook', Eds. M. A. Aegerter, N. Leventis, M. M. Koebel, Springer New York, New York, NY, **2011**, pp. 607-633.
- [69] S. M. Jones, *J. Sol-Gel Sci. Techn.* **2006**, *40*, 351, <https://doi.org/10.1007/s10971-006-7762-7>
- [70] M. Tabata, I. Adachi, Y. Ishii, H. Kawai, T. Sumiyoshi, H. Yokogawa, *Nucl. Instrum. Meth. A* **2010**, *623*, 339, <https://doi.org/10.1016/j.nima.2010.02.241>
- [71] Y. N. Kharzheev, *Phys. Part. Nuclei* **2011**, *39*, 107, <https://doi.org/10.1134/S1063779608010085>
- [72] S. S. Kistler, *Nature* **1931**, *127*, 741, <https://doi.org/10.1038/127741a0>
- [73] S. S. Kistler, *J. Phys. Chem.* **1932**, *36*, 52, <https://doi.org/10.1021/j150331a003>
- [74] L. L. Hench, J. K. West, *Chem. Rev.* **1990**, *90*, 33, <https://doi.org/10.1021/cr00099a003>
- [75] C. J. Brinker, G. W. Scherer, 'Sol-Gel Science: The Physics and Chemistry of Sol-Gel Processing', Academic Press, San Diego, **1990**.
- [76] A. E. Gash, T. M. Tillotson, J. H. Satcher Jr, L. W. Hrubesh, R. L. Simpson, *J. Non-Cryst. Sol.* **2001**, *285*, 22, [https://doi.org/10.1016/S0022-3093\(01\)00427-6](https://doi.org/10.1016/S0022-3093(01)00427-6)
- [77] S. J. Teichner, in 'Aerogels', Ed. J. Fricke, Springer Berlin Heidelberg, Berlin, Heidelberg, **1986**, pp. 22-30.
- [78] F. Rechberger, M. Niederberger, *Nanoscale Horiz.* **2017**, *2*, 6, <https://doi.org/10.1039/C6NH00077K>
- [79] N. Gaponik, A.-K. Herrmann, A. Eychmüller, *J. Phys. Chem. Lett.* **2011**, *3*, 8, <https://doi.org/10.1021/jz201357r>
- [80] M. A. Aegerter, N. Leventis, M. M. Koebel, 'Aerogels Handbook', Springer, Dordrecht, **2011**.
- [81] W. Cheng, F. Rechberger, M. Niederberger, *ACS Nano* **2016**, *10*, 2467, <https://doi.org/10.1021/acsnano.5b07301>
- [82] F. Rechberger, F. J. Heiligtag, M. J. Süess, M. Niederberger, *Angew. Chem. Int. Ed.* **2014**, *53*, 6823, <https://doi.org/10.1002/anie.201402164>
- [83] R. Deshmukh, E. Tervoort, J. Käch, F. Rechberger, M. Niederberger, *Dalton Trans.* **2016**, *45*, 11616, <https://doi.org/10.1039/C6DT01451H>
- [84] J. L. Mohanan, I. U. Arachchige, S. L. Brock, *Science* **2005**, *307*, 397, <https://doi.org/10.1126/science.1104226>
- [85] A. Hitihami-Mudiyanselage, K. Senevirathne, S. L. Brock, *Chem. Mater.* **2014**, *26*, 6251, <https://doi.org/10.1021/cm5030958>
- [86] R. Du, Y. Hu, R. Hübner, J.-O. Joswig, X. Fan, K. Schneider, A. Eychmüller, *Sci. Adv.* **2019**, *5*, eaaw4590, <https://doi.org/10.1126/sciadv.aaw4590>
- [87] F. Rechberger, G. Ilari, C. Willa, E. Tervoort, M. Niederberger, *Mater. Chem. Front.* **2017**, *1*, 1662, <https://doi.org/10.1039/C7QM00155J>
- [88] J. L. Mohanan, S. L. Brock, *J. Non-Cryst. Sol.* **2004**, *350*, 1, <https://doi.org/10.1016/j.jnoncrysol.2004.05.020>
- [89] I. U. Arachchige, S. L. Brock, *J. Am. Chem. Soc.* **2007**, *129*, 1840, <https://doi.org/10.1021/ja066749c>
- [90] Q. Yao, I. U. Arachchige, S. L. Brock, *J. Am. Chem. Soc.* **2009**, *131*, 2800, <https://doi.org/10.1021/ja900042y>
- [91] S. Ganguly, S. L. Brock, *J. Mater. Chem.* **2011**, *21*, 8800, <https://doi.org/10.1039/C1JM11015B>
- [92] S. Ganguly, C. Zhou, D. Morelli, J. Sakamoto, S. L. Brock, *J. Phys. Chem. C* **2012**, *116*, 17431, <https://doi.org/10.1021/jp3055608>
- [93] K. K. Kalebaila, S. L. Brock, *Z. anorg. allg. Chem.* **2012**, *638*, 2598, <https://doi.org/10.1002/zaac.201200354>
- [94] I. R. Pala, S. L. Brock, *ACS Appl. Mater. Interf.* **2012**, *4*, 2160, <https://doi.org/10.1021/am3001538>
- [95] I. K. Hewavitharana, S. L. Brock, *Z. Phys. Chem.* **2018**, *232*, 1691, <https://doi.org/10.1515/zpch-2018-1171>
- [96] C. Rengers, S. V. Voitekovich, S. Kittler, A. Wolf, M. Adam, N. Gaponik, S. Kaskel, A. Eychmüller, *Nanoscale* **2015**, *7*, 12713, <https://doi.org/10.1039/C5NR01880C>
- [97] N. C. Bigall, A.-K. Herrmann, M. Vogel, M. Rose, P. Simon, W. Carrillo-Cabrera, D. Dorfs, S. Kaskel, N. Gaponik, A. Eychmüller, *Angew. Chem. Int. Ed.* **2009**, *48*, 9731, <https://doi.org/10.1002/anie.200902543>
- [98] W. Liu, A.-K. Herrmann, D. Geiger, L. Borchardt, F. Simon, S. Kaskel, N. Gaponik, A. Eychmüller, *Angew. Chem. Int. Ed.* **2012**, *51*, 5743, <https://doi.org/10.1002/anie.201108575>
- [99] D. Wen, A.-K. Herrmann, L. Borchardt, F. Simon, W. Liu, S. Kaskel, A. Eychmüller, *J. Am. Chem. Soc.* **2014**, *136*, 2727, <https://doi.org/10.1021/ja412062e>
- [100] A.-K. Herrmann, P. Formanek, L. Borchardt, M. Klose, L. Giebeler, J. Eckert, S. Kaskel, N. Gaponik, A. Eychmüller, *Chem. Mater.* **2014**, *26*, 1074, <https://doi.org/10.1021/cm4033258>
- [101] R. Du, J. Wang, Y. Wang, R. Hubner, X. Fan, I. Senkovska, Y. Hu, S. Kaskel, A. Eychmüller, *Nat. Commun.* **2020**, *11*, 1590, <https://doi.org/10.1038/s41467-020-15391-w>
- [102] R. O. da Silva, F. J. Heiligtag, M. Karnahl, H. Junge, M. Niederberger, S. Wohlrab, *Catal. Today* **2015**, *246*, 101, <https://doi.org/10.1016/j.cattod.2014.08.028>
- [103] F. J. Heiligtag, M. J. I. Airaghi Leccardi, D. Erdem, M. J. Süess, M. Niederberger, *Nanoscale* **2014**, *6*, 13213, <https://doi.org/10.1039/C4NR04694C>
- [104] F. J. Heiligtag, M. D. Rossell, M. J. Süess, M. Niederberger, *J. Mater. Chem.* **2011**, *21*, 16893, <https://doi.org/10.1039/C1JM11740H>
- [105] F. Rechberger, M. Niederberger, *Mater. Horiz.* **2017**, *4*, 1115, <https://doi.org/10.1039/C7MH00423K>
- [106] A. L. Luna, F. Matter, M. Schreck, J. Wohlwend, E. Tervoort, C. Colbeau-Justin, M. Niederberger, *Appl. Catal. B: Environ.* **2020**, *267*, 118660, <https://doi.org/10.1016/j.apcatb.2020.118660>

- [107] F. Rechberger, E. Tervoort, M. Niederberger, *J. Am. Ceram. Soc.* **2017**, *100*, 4483, <https://doi.org/10.1111/jace.15018>
- [108] M. Odziomek, F. Chaput, F. Lerouge, C. Dujardin, M. Sitarz, S. Karpati, S. Parola, *Chem. Mater.* **2018**, *30*, 5460, <https://doi.org/10.1021/acs.chemmater.8b02443>
- [109] A. Hitihami-Mudiyanselage, K. Senevirathne, S. L. Brock, *ACS Nano* **2013**, *7*, 1163, <https://doi.org/10.1021/nn305959q>
- [110] K. G. S. Ranmohotti, X. Gao, I. U. Arachchige, *Chem. Mater.* **2013**, *25*, 3528, <https://doi.org/10.1021/cm401968j>
- [111] D. Zambo, A. Schlosser, P. Rusch, F. Lubkemann, J. Koch, H. Pfnur, N.C. Bigall, *Small* **2020**, *16*, e1906934, <https://doi.org/10.1002/smll.201906934>
- [112] B. Cai, D. Wen, W. Liu, A.-K. Herrmann, A. Benad, A. Eychmüller, *Angew. Chem. Int. Ed.* **2015**, *54*, 13101, <https://doi.org/10.1002/anie.201505307>
- [113] G. Garnweitner, in 'The Delivery of Nanoparticles', Intechopen.com, **2012**, pp. 71.
- [114] A. Singh, B. A. Lindquist, G. K. Ong, R. B. Jadrich, A. Singh, H. Ha, C. J. Ellison, T. M. Truskett, D. J. Milliron, *Angew. Chem. Int. Ed.* **2015**, *54*, 14840, <https://doi.org/10.1002/anie.201508641>
- [115] V. Sayevich, B. Cai, A. Benad, D. Haubold, L. Sonntag, N. Gaponik, V. Lesnyak, A. Eychmüller, *Angew. Chem. Int. Ed.* **2016**, *55*, 6334, <https://doi.org/10.1002/anie.201600094>
- [116] V. Lesnyak, S. V. Voitekhovich, P. N. Gaponik, N. Gaponik, A. Eychmüller, *ACS Nano* **2010**, *4*, 4090, <https://doi.org/10.1021/nn100563c>
- [117] W. Cheng, F. Rechberger, M. Niederberger, *Nanoscale* **2016**, *8*, 14074, <https://doi.org/10.1039/C6NR04429H>
- [118] C. C. Hewa-Rahinduwage, X. Geng, K. L. Silva, X. Niu, L. Zhang, S. L. Brock, L. Luo, *J. Am. Chem. Soc.* **2020**, *142*, 12207, <https://doi.org/10.1021/jacs.0c03156>
- [119] Q. Yao, S. L. Brock, *Nanotechnology* **2010**, *21*, 115502, <https://doi.org/10.1088/0957-4484/21/11/115502>
- [120] L. Nahar, A. A. Farghaly, R. J. A. Esteves, I. U. Arachchige, *Chem. Mater.* **2017**, *29*, 7704, <https://doi.org/10.1021/acs.chemmater.7b01731>
- [121] D. Wen, W. Liu, D. Haubold, C. Zhu, M. Oschatz, M. Holzschuh, A. Wolf, F. Simon, S. Kaskel, A. Eychmüller, *ACS Nano* **2016**, *10*, 2559, <https://doi.org/10.1021/acs.nano.5b07505>
- [122] H. Wang, S. Zhang, W. Cai, B. Z. Xu, Z. Cai, Y. Wu, X. Luo, X. Wei, Z. Liu, W. Gu, A. Eychmüller, C. Zhu, J. Chen, *Mater. Horiz.* **2020**, *7*, 2407, <https://doi.org/10.1039/D0MH00646G>
- [123] X. Fan, S. Zerebecki, R. Du, R. Hubner, G. Marzum, G. Jiang, Y. Hu, S. Barcikowski, S. Reichenberger, A. Eychmüller, *Angew. Chem. Int. Ed.* **2010**, *59*, 5706, <https://doi.org/10.1002/anie.201913079>
- [124] R. Du, J. O. Joswig, X. Fan, R. Hubner, D. Spittel, Y. Hu, A. Eychmüller, *Matter* **2020**, *2*, 908, <https://doi.org/10.1016/j.matt.2020.01.002>
- [125] W. Liu, P. Rodriguez, L. Borchardt, A. Foelske, J. Yuan, A.-K. Herrmann, D. Geiger, Z. Zheng, S. Kaskel, N. Gaponik, R. Kötz, T. J. Schmidt, A. Eychmüller, *Angew. Chem. Int. Ed.* **2013**, *52*, 9849, <https://doi.org/10.1002/anie.201303109>
- [126] S. Henning, L. Kuhn, J. Herranz, J. Durst, T. Binninger, M. Nachttegaal, M. Werheid, W. Liu, M. Adam, S. Kaskel, A. Eychmüller, T. J. Schmidt, *J. Electrochem. Soc.* **2016**, *163*, F998, <https://doi.org/10.1149/2.0251609jes>
- [127] B. Cai, R. Hübner, K. Sasaki, Y. Zhang, D. Su, C. Ziegler, M. B. Vukmirovic, B. Rellinghaus, R. R. Adzic, A. Eychmüller, *Angew. Chem.* **2017**, *57*, 2963, <https://doi.org/10.1002/ange.201710997>
- [128] M. Oezaslan, A. K. Herrmann, M. Werheid, A. I. Frenkel, M. Nachttegaal, C. Dosche, L. B. A. Celine, H. C. Yilmaz, L. Kuehn, E. Rhiel, N. Gaponik, A. Eychmüller, T. J. Schmidt, *ChemCatChem* **2017**, *9*, 798, <https://doi.org/10.1002/cctc.201600667>
- [129] M. Oezaslan, W. Liu, M. Nachttegaal, A. I. Frenkel, B. Rutkowski, M. Werheid, A. K. Herrmann, C. Laugier-Bonnaud, H.C. Yilmaz, N. Gaponik, A. Czyska-Filemonowicz, A. Eychmüller, T. J. Schmidt, *Phys. Chem. Chem. Phys.* **2016**, *18*, 20640, <https://doi.org/10.1039/C6CP03527B>
- [130] R. Du, W. Jin, R. Hübner, L. Zhou, Y. Hu, A. Eychmüller, *Adv. Ener. Mater.* **2020**, *10*, <https://doi.org/10.1002/aenm.201903857>

#### License and Terms



This is an Open Access article under the terms of the Creative Commons Attribution License CC BY 4.0. The material may not be used for commercial purposes.

The license is subject to the CHIMIA terms and conditions: (<http://chimia.ch/component/sppagebuilder/?view=page&id=12>).

The definitive version of this article is the electronic one that can be found at <https://doi.org/10.2533/chimia.2021.387>